

# A Self-Assembled Fluoride–Water Cyclic Cluster of $[\text{F}(\text{H}_2\text{O})_4]^{4-}$ in a Molecular Box

Md. Alamgir Hossain,<sup>\*,†</sup> Musabbir A. Saeed,<sup>†</sup> Avijit Pramanik,<sup>†</sup> Bryan M. Wong,<sup>‡</sup> Syed A. Haque,<sup>†</sup> and Douglas R. Powell<sup>§</sup>

<sup>†</sup>Department of Chemistry and Biochemistry, Jackson State University, Jackson, Mississippi 39217, United States

<sup>‡</sup>Materials Chemistry Department, Sandia National Laboratories, Livermore, California 94551, United States

<sup>§</sup>Department of Chemistry and Biochemistry, University of Oklahoma, Norman, Oklahoma 73019, United States

## S Supporting Information

**ABSTRACT:** We present an unprecedented fluoride–water cyclic cluster of  $[\text{F}(\text{H}_2\text{O})_4]^{4-}$  assembled in a cuboid molecular box formed by two large macrocycles. Structural characterization reveals that  $[\text{F}(\text{H}_2\text{O})_4]^{4-}$  is assembled by strong H-bonding interactions [ $\text{OH}\cdots\text{F} = 2.684(3)–2.724(3)$  Å], where a fluoride anion plays the topological role of a water molecule in the classical cyclic water octamer. The interaction of fluoride was further confirmed by <sup>19</sup>F NMR and <sup>1</sup>H NMR spectroscopies, indicating the encapsulation of the anionic species within the cavity in solution. High-level DFT calculations and Bader topological analyses fully support the crystallographic results, demonstrating that the bonding arrangement in the fluoride–water cluster arises from the unique geometry of the host.

Ordered self-assembly involves spontaneous association of molecular species under certain conditions to generate highly structured aggregates stabilized by non-covalent interactions. The molecular interactions between fluoride anions and chemical receptors continue to be of particular interest due to their significance in environmental, biological, and health-related processes.<sup>1–14</sup> For example, the presence of fluoride anions in drinking water has been known to significantly impact human health, with direct effects on dental and skeletal fluorosis.<sup>1–3</sup> A fluoride–water adduct,  $[\text{F}(\text{H}_2\text{O})]^-$ , also plays an important role in the stabilization of certain heme proteins such as ferric sperm whale myoglobin, where the fluoride anion is coordinated with one water, a distal His64E7NE2 atom, and the heme iron.<sup>15</sup> Here we report a novel self-assembled  $[\text{F}(\text{H}_2\text{O})_4]^{4-}$  cluster formed in a cuboid molecular box provided by two parallel hosts, two water molecules, and two silicon hexafluoride anions ( $\text{SiF}_6^{2-}$ ). In this self-contained molecular box, the unique geometry of the surrounding host provides an ideal microenvironment for assembling large hydrated guests.

The smallest member in the halide series, the fluoride anion is distinct from its congeners, displaying a high electronegativity and hydration energy.<sup>16</sup> This tiny anion has a high tendency to be hydrated instead of being isolated, making it even more challenging to bind with synthetic hosts in water. Cametti and Rissanen recognized that a “hydrated fluoride” has more

relevance and importance than a “naked fluoride anion” within the anion recognition arena.<sup>17</sup> Although a hydrated fluoride has been the subject of extensive theoretical studies,<sup>18–23</sup> experimental evidence of a fluoride–water cluster inside an enclosed cavity is remarkably lacking.<sup>11,24–26</sup> The recognition of hydrated fluoride was reported by Bowman-James et al., describing the encapsulation of  $[\text{F}(\text{H}_2\text{O})]^-$  in an *m*-xylyl-based cryptand,<sup>24</sup>  $[\text{F}(\text{H}_2\text{O})\text{F}]^{2-}$  in a slightly expanded *p*-xylyl-based cryptand,<sup>25</sup> and  $[\text{F}(\text{H}_2\text{O})_4]^-$  in an amide-based tetrahedral host,<sup>26</sup> with the fluoride anion tetrahedrally coordinated within a single molecule in each case. Recently, Ghosh et al. reported the formation of hydrated fluorides as  $[\text{F}_4(\text{H}_2\text{O})_{10}]^{4-}$  stabilized inside an amide-based capsule.<sup>11</sup> Such an assembled fluoride–water cyclic cluster within a closed nanocavity has not previously been observed.

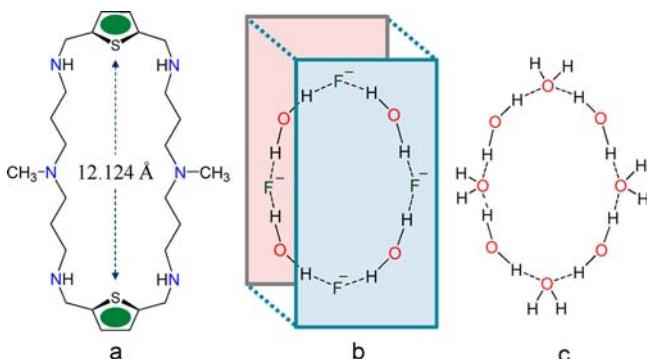
In 2001, Atwood et al. reported a cyclic  $(\text{H}_2\text{O})_8$  cluster, where four water molecules serve as two H-bond donors and the remaining four as two acceptors.<sup>27</sup> In 2011, we reported that  $\text{R}_2\text{NH}_2^+$  with H-bond donors and  $\text{H}_2\text{PO}_4^-$  with both H-bond donors and acceptors can be successfully used in place of a water molecule for the formation of an amine–water cyclic cluster,  $[\text{NH}_2^+(\text{H}_2\text{O})_4]^{28}$  and a dihydrogen phosphate octamer,  $[(\text{H}_2\text{PO}_4^-)_8]^{29}$ . Here we report a self-assembled fluoride–water cyclic tetramer,  $[\text{F}(\text{H}_2\text{O})_4]^{4-}$ , fully enclosed in a cuboid-type molecular box comprising two large (12.124 Å long) parallel macrocycles. The fluoride anions and water molecules are H-bonded to each other in an alternating fashion within the fluoride–water hybrid cluster, where a fluoride anion plays the topological role of a water molecule in the classical cyclic water octamer  $(\text{H}_2\text{O})_8$  (Chart 1).

Receptor L was synthesized from the reaction of an equimolar amount of *N*-methyl-3,3'-diaminodipropylamine and 2,5-thiophenedicarbaldehyde under high dilution conditions in  $\text{CH}_3\text{OH}$  followed by reduction with  $\text{NaBH}_4$ .<sup>30</sup> The fluoride salt was obtained as a white powder after addition of aqueous HF to L in  $\text{CH}_3\text{OH}$  in a Teflon vial. Attempts to grow crystals of the fluoride salt in a Teflon vial, to avoid possible contamination with  $\text{SiF}_6^{2-}$  anions from a glass container,<sup>24,25</sup> were unsuccessful. We therefore grew crystals in a glass vial by slow evaporation of a  $\text{CH}_3\text{OH}/\text{H}_2\text{O}$  solution of the fluoride salt, providing colorless prism-shaped crystals as  $[\text{H}_6\text{L}-$

Received: May 6, 2012

Published: July 5, 2012

**Chart 1. (a) Receptor L, (b) Fluoride–Water Hybrid Tetramer  $[\text{F}(\text{H}_2\text{O})_4]^{4-}$  in a Molecular Box, and (c) Cyclic Water Octamer Formed by Four Water Molecules as H-Bond Donors and Four Water Molecules as H-Bond Acceptors**



$(\text{F})_2(\text{H}_2\text{O})_2]^{4+} \cdot 2(\text{SiF}_6^{2-}) \cdot 8(\text{H}_2\text{O})$ .<sup>31</sup> One  $\text{SiF}_6^{2-}$  and two water sites outside the cavity were disordered and best modeled using the Squeeze program.<sup>32</sup>

Structural analysis of the fluoride complex reveals that fluoride anions are assembled with water molecules in a highly ordered H-bonding network to form a fluoride–water cyclic tetramer,  $[\text{F}(\text{H}_2\text{O})_4]^{4-}$ , between two hexaprotonated macrocycles. Each macrocycle adopts a rectangular shape, and the two thiophene rings in a macrocyclic unit are oriented parallel to each other, with  $\text{Ar}_{\text{centroid}} \cdots \text{Ar}_{\text{centroid}} = 12.124 \text{ \AA}$ . Figure 1a shows

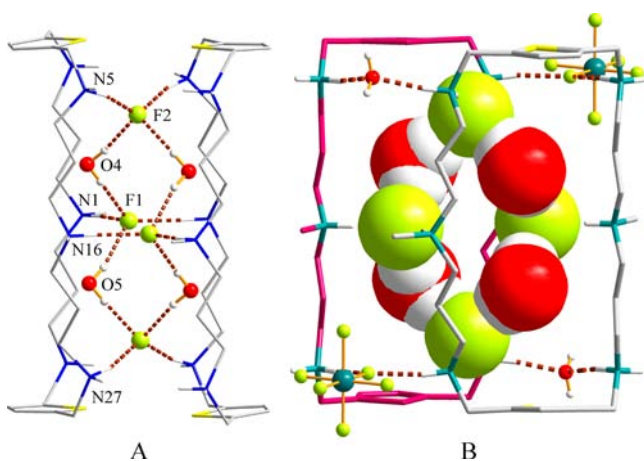


**Figure 1.** Crystal structure of the fluoride complex. (a) Side view showing the water–fluoride tetramer,  $[\text{F}(\text{H}_2\text{O})_4]^{4-}$ , between the two macrocycles. (b) Space-filling view of  $[\text{F}(\text{H}_2\text{O})_4]^{4-}$  in a molecular box formed by two parallel macrocycles, two water molecules, and two silicon hexafluorides.

that each fluoride is coordinated with two NH groups from two macrocycles and with two water molecules, completing  $[\text{F}(\text{H}_2\text{O})_4]^{4-}$  between the two parallel macrocycles. Each fluoride is strongly bonded with four H-bond-donors in a tetrahedral coordination geometry, as previously observed in Lehn's BISTREN for naked fluoride.<sup>33</sup> The H-bonding interactions of  $\text{NH} \cdots \text{F}$  and  $\text{OH} \cdots \text{F}$  ranging from 2.587(3)–2.628(3) and 2.684(3)–2.724(3) Å, respectively (Table 1). The corresponding distances are comparable to those reported for the fluoride complex of *p*-xylyl cryptand ( $\text{NH} \cdots \text{F} = 2.65 \text{ \AA}$ )<sup>25</sup> and for the fluoride–water cluster  $[\text{F}(\text{H}_2\text{O})]^-$  inside the

**Table 1. H-Bonding Parameters (Distances in Å, Angles in deg) for the Fluoride Complex of L**

D–H $\cdots$ F	H $\cdots$ F	D $\cdots$ F	$\angle$ DHF
N1–H1 $\cdots$ F1	1.71	2.628(3)	166.7
N5–H5A $\cdots$ F2	1.71	2.614(3)	165.7
N16–H16 $\cdots$ F1 <sup>a</sup>	1.69	2.614(3)	169.6
N27–H27B $\cdots$ F2 <sup>a</sup>	1.68	2.587(3)	167.0
O4–H4OA $\cdots$ F1	1.94	2.724(3)	166.7
O4–H4OB $\cdots$ F2 <sup>a</sup>	1.89	2.684(3)	172.5
O4–H4OA $\cdots$ F1	1.94	2.724(3)	166.7
O5–H5OB $\cdots$ F2	1.94	2.724(3)	167.1

<sup>a</sup>Symmetry code:  $-x + 1, -y + 1, -z + 1$ .

ferric sperm whale myoglobin ( $\text{NH} \cdots \text{F} = 2.74 \text{ \AA}$  and  $\text{OH} \cdots \text{F} = 2.71 \text{ \AA}$ ).<sup>15</sup> In the cyclic cluster, four fluorides act as double H-bond acceptors and four water molecules as double H-bond donors. The bonding patterns are surprisingly similar to that for the cyclic  $(\text{H}_2\text{O})_8$  cluster reported by Atwood et al.,<sup>27</sup> with four water molecules as donors and four water molecules as acceptors (see Chart 1c). In addition to the formation of a fluoride–water cyclic cluster, two macrocycles are further connected with two water molecules and two silicon hexafluorides via NH protons ( $\text{NH} \cdots \text{O} = 2.698(4)$  and  $2.685(5) \text{ \AA}$ ;  $\text{NH} \cdots \text{F} = 2.708(4)$ – $3.004(4) \text{ \AA}$ ), respectively, resulting in a cuboid-type molecular box. Clearly, both the silicon hexafluorides and water molecules play an important structural role in holding the two macrocycles together through H-bonding interactions. A space-filling view (Figure 1b) illustrates the compact arrangement of this water–fluoride cyclic tetramer stabilized in the molecular box. It is worth mentioning that all fluoride anions in the complex are fully utilized for the cluster formation in the solid state.

<sup>19</sup>F NMR spectroscopy was used to characterize the chemical environment of fluoride anions in the presence of  $[\text{H}_6\text{L}](\text{Ts})_6$  [ $\text{Ts} = p$ -toluenesulfonate] in water. For this purpose, <sup>19</sup>F NMR spectra were recorded for the fluoride solution (5 mM *n*-tetrabutylammonium fluoride (*n*-Bu<sub>4</sub>NF) in D<sub>2</sub>O) before and after addition of the host (50 mM in D<sub>2</sub>O) at pH 2.0. To make a direct comparison, the same solution of TBAF (5 mM in D<sub>2</sub>O) was used as an external reference in a sealed capillary tube and placed in the NMR tube. As clearly shown in Figure 2, the signal at  $\delta_{\text{F}} = -122.3 \text{ ppm}$  assigned to the unbound fluoride significantly shifts upfield to  $-141.8 \text{ ppm}$  ( $\Delta\delta = 29.5 \text{ ppm}$ ) due to the addition of 5 equiv of  $[\text{H}_6\text{L}](\text{Ts})_6$ , indicating the encapsulation of fluoride in the cavity. Furthermore, a new peak emerges at  $-127.9 \text{ ppm}$  that remains unchanged during the titration process (Figure 2b–e). This peak could be assigned to  $\text{SiF}_6^{2-}$ <sup>34,35</sup> and is formed due to the addition of TBAF at low pH. The formation of  $\text{SiF}_6^{2-}$  is quite common, particularly in the presence of HF or fluoride salts,<sup>36</sup> and is also consistent with the results of our crystallographic data. However, upon addition of NaOD to the solution of TBAF containing 5 equiv of the host (Figure 2e), two significant changes were observed: the peak at  $\delta_{\text{F}} = -127.9 \text{ ppm}$  disappeared, and the peak at  $\delta_{\text{F}} = 133.8 \text{ ppm}$  shifted downfield to  $-122.0 \text{ ppm}$ . The disappearance of the peak at  $-127.9 \text{ ppm}$  for  $\text{SiF}_6^{2-}$  could be due to the reaction  $\text{SiF}_6^{2-} + \text{NaOH} \rightarrow \text{NaF} + \text{SiO}_2 + \text{H}_2\text{O}$  (used in water fluoridation).<sup>37</sup> However, the huge upfield shift close to the unbound fluoride ( $-122.3 \text{ ppm}$ ) could be the result of the decomplexation of fluoride at higher pH ( $\sim 7.0$ ), as expected.

<sup>1</sup>H NMR titration studies were performed to evaluate the binding affinity of  $[\text{H}_6\text{L}](\text{Ts})_6$  to various anions of *n*-Bu<sub>4</sub>N<sup>+</sup>

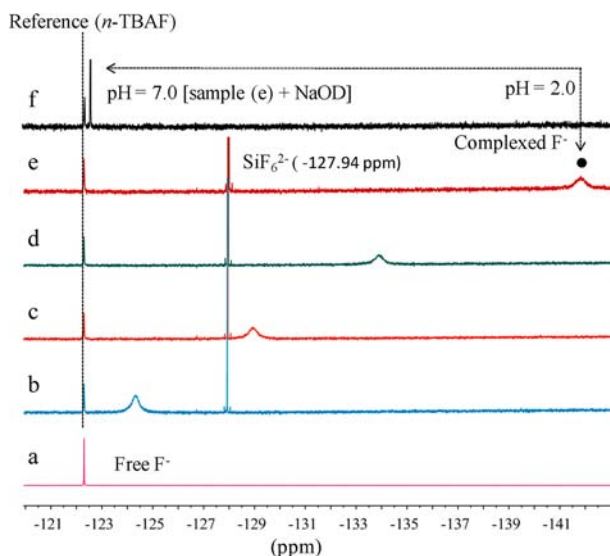


**Figure 2.**  $^{19}\text{F}$  NMR spectra of  $n\text{-Bu}_4\text{N}^+\text{F}^-$  in  $\text{D}_2\text{O}$  recorded at room temperature: (a) free  $n\text{-Bu}_4\text{N}^+\text{F}^-$  ( $\delta_{\text{F}} = -122.3$  ppm); (b)  $n\text{-Bu}_4\text{N}^+\text{F}^- + 1.5$  equiv of  $[\text{H}_6\text{L}](\text{Ts})_6$  ( $-124.3$  ppm); (c)  $n\text{-Bu}_4\text{N}^+\text{F}^- + 2.5$  equiv of  $[\text{H}_6\text{L}](\text{Ts})_6$  ( $-128.9$  ppm); (d)  $n\text{-Bu}_4\text{N}^+\text{F}^- + 3.5$  equiv of  $[\text{H}_6\text{L}](\text{Ts})_6$  ( $-133.8$  ppm); (e)  $n\text{-Bu}_4\text{N}^+\text{F}^- + 5.0$  equiv of  $[\text{H}_6\text{L}](\text{Ts})_6$  ( $-141.8$  ppm); and (f) after adding NaOD to the sample (e) [pH 7.0].

salts in  $\text{DMSO}-d_6$ . The addition of  $n\text{-Bu}_4\text{NF}$  to the host resulted in an upfield shift of both  $\text{ArH}$  and  $\text{CH}_2$  resonances of the macrocycle (Figure S8). Our results show that the receptor exhibits the strongest interaction with  $\text{F}^-$  over other anions (Table 2), providing the best fit to a 1:2 (L:A) binding mode.<sup>38</sup>

**Table 2. Binding Constants (in  $\log K$ ) for the Receptor  $[\text{H}_6\text{L}](\text{Ts})_6$  with Anions in  $\text{DMSO}-d_6$  Containing 0.025% Water at 25 °C**

$\text{F}^-$	1.92(2), 3.48(2) <sup>a</sup>	$\text{NO}_3^-$	1.72(1)
$\text{Cl}^-$	2.14(1)	$\text{ClO}_4^-$	<1
$\text{Br}^-$	1.96(3)	$\text{HSO}_4^-$	2.23(2)
$\text{I}^-$	<1	$\text{H}_2\text{PO}_4^-$	<sup>b</sup>

<sup>a</sup>Binding constant for a 1:2 (L:A) binding model. All other binding constants given in this table represent a 1:1 binding (L:A). <sup>b</sup>NMR titration was hampered by precipitation upon addition of the anion.

The 1:2 stoichiometry was confirmed by a Job plot analysis;<sup>39</sup> however, the host was found to form a 1:1 complex with a larger anion, which could be due to its size. Surprisingly, the 1:2 binding constants increased with the water fraction (0.025 to 5%, see Table S1). This trend is opposite to what is generally expected in a more polar solvent like water, where H-bonding ability of the host is lessened.<sup>40</sup> This trend may be due to participation of water with the bonded fluorides as observed in the X-ray structure. The concentration-dependent  $^1\text{H}$  NMR spectra, upon dilution of  $[\text{H}_6\text{L}](\text{Ts})_6$  in the presence of 5 equiv of  $n\text{-Bu}_4\text{NF}$  in  $\text{DMSO}-d_6/0.025$  water, suggest the formation of a dimer in solution ( $K_{\text{dim}} = 46 \text{ M}^{-1}$ ), in agreement with the crystallographic results. A similar dimerization was observed by Haley, Johnson, et al. for pyridine-based sulfonamides with water or chloride.<sup>41</sup> While the concentration of water was increased to 5.0%, the dimerization constant was higher ( $K_{\text{dim}} = 126 \text{ M}^{-1}$ ) than that observed in  $\text{DMSO}-d_6/0.025\%$  water. This

observation further supports the possible involvement of water molecules in the binding process.

To quantitatively understand the unique assembly of the fluoride–water cluster within the molecular box, density functional theory (DFT) calculations were performed on the enclosed  $[\text{F}(\text{H}_2\text{O})_4]^{4-}$  species between the two macrocycles in the absence and in the presence of linking groups ( $\text{H}_2\text{O}$  and  $\text{SiF}_6^{2-}$ ). All quantum chemical calculations were carried out with the M06-2X hybrid functional, which we have previously shown to accurately predict the binding energies of water and ions within large molecular systems.<sup>28,29,42</sup> All molecular geometries were completely optimized without constraints at the M06-2X/6-31G(d,p) level of theory in the presence of a polarizable continuum model (PCM) solvent model to approximate an aqueous environment (dielectric constant = 78.4). From the DFT-optimized geometries, we calculated the cohesive energies ( $=E_{\text{anions}} + 2E_{\text{ligand}} - E_{\text{total complex}}$ ) of both complexes. While both systems provided stable fluoride–water clusters (see Supporting Information for optimized geometries and total energies), it is interesting to note that the complex with the  $[\text{F}(\text{H}_2\text{O})_4]^{4-}$  species in the molecular box formed by two macrocycles, two linking  $\text{H}_2\text{O}$  groups, and two linking  $\text{SiF}_6^{2-}$  ions is energetically more favorable (25.4 kcal/mol) than the complex without the linking groups (18.6 kcal/mol). The bonding patterns in the complex are quite similar (Figure 3) to those observed in the X-ray data (*vide supra*).

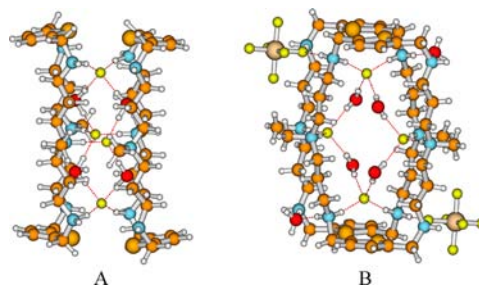


**Figure 3.** Optimized DFT geometry of  $[\text{F}(\text{H}_2\text{O})_4]^{4-}$  (a) between the two hosts and (b) in the molecular box formed by two hosts, two water molecules, and two silicon hexafluorides.

To characterize the unique topological properties of the electron density distribution even further, we also used Bader's Quantum Theory of Atoms-In-Molecules (QTAIM) approach to calculate bond critical points (BCPs) throughout the complex.<sup>43</sup> Within this formalism, the presence of a BCP as well as a positive value of the Laplacian of the density ( $\nabla^2\rho$ ) at the BCP gives a quantitative measure of the strength of a particular bond. Within our enclosed water cluster, we found that all of the H-bonds in both the  $\text{N}-\text{H}\cdots\text{F}$  and  $\text{O}-\text{H}\cdots\text{F}$  groups are quite strong, with large positive values. However, our QTAIM analysis indicates that the  $\text{N}-\text{H}\cdots\text{F}$  bonds are considerably stronger, with  $\nabla^2\rho = 0.20$ , while all the other  $\text{O}-\text{H}\cdots\text{F}$  bonds are weaker, with  $\nabla^2\rho < 0.13$ . The relative strengths of these H-bonds reflect the different electronegativities of the heteroatom (also in agreement with our QTAIM charge population analysis) and highlight the important role of the relative orientation of the  $\text{N}-\text{H}$  functional groups in the box.

In conclusion, we have presented the assembly of a fluoride–water cyclic tetramer  $[\text{F}(\text{H}_2\text{O})_4]^{4-}$  within a molecular box comprised of a pair of large macrocyclic frameworks. Each macrocycle is preorganized in such a way as to donate

directional H-bonds for fluoride anions and to provide a precise space for water molecules, resulting in the formation of a fluoride–water hybrid cluster. Four fluoride anions and four water molecules are assembled in an alternating fashion to form an octameric cycle, where fluorides play the topological role of water molecules in the classical octameric water cluster (H<sub>2</sub>O)<sub>8</sub>.<sup>27</sup> The assembly of the stable fluoride–water cluster is fully supported by high-level DFT calculations and Bader topological analyses, demonstrating that the unique assembly of the fluoride–water cluster results from the precisely positioned binding sites in the macrocycles as well as the linking water and hexafluoride species. In addition to presenting an exceptional example of a highly organized anion–water cyclic tetramer in a large cavity, this modular approach based on a large host leads to promising new types of self-assembled structures and is a step toward understanding the complex aqueous-phase environment of an anion. Such self-assembled clusters inside a closed cavity may be useful for the generation of novel functional materials.<sup>44</sup> Further studies on the assembly of other anion clusters with this macrocycle and related compounds are currently in progress.

## ■ ASSOCIATED CONTENT

### ■ Supporting Information

Crystallographic data (CIF); <sup>1</sup>H, <sup>13</sup>C and 2D NOESY NMR, NMR titration spectra, dilution experiments, additional structures of the fluoride complex, Cartesian coordinates of optimized structures, and electronic energies. This material is available free of charge via the Internet at <http://pubs.acs.org>.

## ■ AUTHOR INFORMATION

### Corresponding Author

alamgir.hossain@jsums.edu

### Notes

The authors declare no competing financial interest.

## ■ ACKNOWLEDGMENTS

The National Science Foundation is acknowledged for a CAREER award (CHE-1056927) to M.A.H. This work was supported by the National Institutes of Health (G12RR013459). The authors thank the National Science Foundation (CHE-0130835) and the University of Oklahoma for funds to acquire the diffractometer used in this work.

## ■ REFERENCES

- (1) Hudnall, T. W.; Chiu, C.-W.; Gabbai, F. P. *Acc. Chem. Res.* **2009**, *42*, 388.
- (2) Dietrich, B.; Lehn, J.-M.; Guilhem, J.; Pascard, C. *Tetrahedron Lett.* **1989**, *30*, 4125.
- (3) Zhang, B.; Cai, P.; Duan, C.; Miao, R.; Zhu, L.; Niitsu, T.; Inoue, H. *Chem. Commun.* **2004**, 2206.
- (4) Woods, C. J.; Camiolo, S.; Light, M. E.; Coles, S. J.; Hursthouse, M. B.; King, M. A.; Galenand, P. A.; Essex, J. W. *J. Am. Chem. Soc.* **2002**, *124*, 8644.
- (5) Kang, S. O.; Llinares, J. M.; Powell, D.; VanderVelde, D.; Bowman-James, K. *J. Am. Chem. Soc.* **2003**, *125*, 10152.
- (6) Kang, S. O.; VanderVelde, D.; Powell, D.; Bowman-James, K. *J. Am. Chem. Soc.* **2004**, *126*, 12272.
- (7) Ilioudis, C. A.; Tocher, D. A.; Steed, J. W. *J. Am. Chem. Soc.* **2004**, *126*, 12395.
- (8) Mascal, M.; Yakovlev, I.; Nikitin, E. B.; Fettingner, J. C. *Angew. Chem., Int. Ed.* **2007**, *46*, 8782.
- (9) Bates, G. W.; Gale, P. A.; Light, M. E. *Chem. Commun.* **2007**, 2121.

- (10) Arunachalam, M.; Ghosh, P. *Chem. Commun.* **2009**, 5389.
- (11) Arunachalam, M.; Ghosh, P. *Chem. Commun.* **2011**, 47, 6269.
- (12) Kang, S. O.; Day, V. W.; Bowman-James, K. *J. Org. Chem.* **2010**, *75*, 277.
- (13) Dalapati, S.; Alam, M. A.; Saha, R.; Jana, S.; Guchhait, N. *CrystEngComm.* **2012**, *14*, 1527.
- (14) Pramanik, A.; Powell, D. R.; Wong, B. M.; Hossain, M. A. *Inorg. Chem.* **2012**, *51* (7), 4274.
- (15) Aime, S.; Fasano, M.; Paoletti, S.; Cutruzzola, F.; Desideri, A.; Bolognesi, M.; Rizzi, M.; Ascenzi, P. *Biophys. J.* **1996**, *70*, 482.
- (16) Zhan, C.-G.; Dixon, D. A. *J. Phys. Chem. A* **2004**, *108*, 2020.
- (17) Cametti, M.; Rissanen, K. *Chem. Commun.* **2009**, 2809.
- (18) Bryce, R. A.; Vincent, M. A.; Hillier, I. H. *J. Phys. Chem. A* **1999**, *103*, 4094.
- (19) Weis, P.; Kemper, P. R.; Bowers, M. T.; Xantheas, S. S. *J. Am. Chem. Soc.* **1999**, *121*, 3531.
- (20) Lee, H. M.; Kim, D.; Kima, K. S. *J. Chem. Phys.* **2002**, *116*, 5509.
- (21) Kemp, D. D.; Gordon, M. S. *J. Phys. Chem. A* **2005**, *109*, 7688.
- (22) Kelly, C. P.; Cramer, C. J.; Truhlar, D. G. *J. Phys. Chem. B* **2006**, *110*, 16066.
- (23) Lima, S.; Goodfellow, B. J.; Teixeira-Dias, J. J. C. *J. Inclusion Phenom. Macrocycl. Chem.* **2006**, *54*, 35.
- (24) Mason, S.; Llinares, J. M.; Morton, M.; Clifford, T.; Bowman-James, K. *J. Am. Chem. Soc.* **2000**, *122*, 1814.
- (25) Hossain, M. A.; Llinares, J. M.; Mason, S.; Morehouse, P.; Powell, D.; Bowman-James, K. *Angew. Chem., Int. Ed.* **2002**, *41*, 2335.
- (26) Wang, Q.-Q.; Day, V. W.; Bowman-James, K. B. *Angew. Chem., Int. Ed.* **2012**, *51*, 2119.
- (27) Atwood, J. L.; Barbour, L. J.; Ness, T. J.; Raston, C. L.; Raston, P. L. *J. Am. Chem. Soc.* **2001**, *123*, 7192.
- (28) Saeed, M. A.; Wong, B. M.; Fronczek, F. R.; Venkatraman, R.; Hossain, M. A. *Cryst. Growth Des.* **2010**, *10*, 1486.
- (29) Işıklan, M.; Saeed, M. A.; Pramanik, A.; Wong, B. M.; Fronczek, F. R.; Hossain, M. A. *Cryst. Growth Des.* **2011**, *11*, 959.
- (30) Chen, D.; Martell, A. E. *Tetrahedron* **1991**, *47*, 6900.
- (31) Crystal data for C<sub>26</sub>H<sub>52</sub>N<sub>6</sub>S<sub>2</sub>·2SiF<sub>6</sub><sup>2-</sup>·2F<sup>-</sup>·10(H<sub>2</sub>O): *M* = 1015.20, triclinic, *a* = 12.419(2) Å, *b* = 13.116(2) Å, *c* = 15.871(3) Å, *α* = 66.443(4)°, *β* = 88.215(4)°, *γ* = 71.224(5)°, *V* = 2229.4(6) Å<sup>3</sup>, *T* = 100(2) K, space group *P* $\bar{1}$ , *Z* = 2, *μ*(Mo *Kα*) = 0.286 mm<sup>-1</sup>, 36 190 reflections measured, 8772 independent reflections (*R*<sub>int</sub> = 0.0622); *R*1 = 0.0669 (*I* > 2 $\sigma$ (*I*)), *R*1 = 0.0926 (all data)
- (32) van der Sluis, Spek, P. A. L. *Acta Crystallogr.* **1990**, *A46*, 194.
- (33) Dietrich, B.; Dilworth, B.; Lehn, J.-M.; Souchez, J.-P.; Cesario, M.; Guilhem, J.; Pascard, C. *Helv. Chim. Acta* **1996**, *79*, 569.
- (34) Christe, K. O.; Wilson, W. W. *J. Fluorine Chem.* **1990**, *46*, 339.
- (35) Gupta, N. S.; Wragg, D. S.; Tilsetc, M.; Omtvedt, J. P. *Acta Crystallogr.* **2011**, *E67*, o1958.
- (36) Anderson, K. M.; Goeta, A. E.; Hancock, K. S. B.; Steed, J. W. *Chem. Commun.* **2006**, 2138.
- (37) Aigueperse, J.; Mollard, P.; Devilliers, D.; Chemla, M.; Faron, R.; Romano, R.; Cuer, J. P. Fluorine Compounds, Inorganic In *Ullmann's Encyclopedia of Industrial Chemistry*; Wiley-VCH: Weinheim, 2005.
- (38) Hynes, M. J. *J. Chem. Soc., Dalton Trans.* **1993**, 311.
- (39) Mendy, J. S.; Pilate, M. L.; Horne, T.; Day, V. W.; Hossain, M. A. *Chem. Commun.* **2010**, 46, 6084.
- (40) Choi, K.; Hamilton, A. D. *J. Am. Chem. Soc.* **2003**, *125*, 10241.
- (41) Berryman, O. B.; Johnson, C. A., II; Zakharov, L. N.; Haley, M. M.; Johnson, D. W. *Angew. Chem., Int. Ed.* **2008**, *47*, 117.
- (42) Saeed, M. A.; Pramanik, A.; Wong, B. M.; Haque, S. A.; Powell, D. R.; Chand, D. K.; Hossain, M. A. *Chem. Commun.* **2012**, DOI: 10.1039/C2CC30767G.
- (43) Bader, R. *Chem. Rev.* **1991**, *91*, 893.
- (44) Chaur, M. N.; Melin, F.; Ortiz, A. L.; Echegoyen, L. *Angew. Chem., Int. Ed.* **2009**, *48*, 7514.